Impedance Control of a Redundant Parallel Manipulator

Juan de Dios Flores Mendez[1], Henrik Schiøler[1], Ole Madsen[2] and Shaoping Bai[2]

[1]*Department of Electronic Systems, Aalborg University, Frederik Bajers Vej 7C, 9220, Aalborg East, Denmark*
[2]*Department of Mechanical and Manufacturing Engineering, Aalborg University,*
Fibigerstraede 16, 9220, Aalborg East, Denmark

Keywords: Robotics, Redundant Parallel Manipulators, Control, Optimization, Compliant Motion, Impedance Control.

Abstract: This paper presents the design of Impedance Control to a redundantly actuated Parallel Kinematic Manipulator. The proposed control is based on treating each limb as a single system and their connection through the internal interaction forces. The controller introduces a stiffness and damping matrices that decouples the dynamic behaviour of the robot. Control allocation of torques is applied through an optimization that promotes even distribution of torques over actuators. Simulations showed a good compliance behaviour in low frequencies.

1 INTRODUCTION

Parallel Kinematic Manipulators (**PKMs**) have been mainly used in pick and place operations or positioning systems in manufacturing due to their high speed, high accelerations and low inertia (Patel and George, 2012), with applications such as assembly (McCallion and Pham, 1979), positioning (Ming and Higuchi, 1994), motion simulators (Salcudean et al., 1994), pick and place (Powell, 1982), and material processing operations such as drilling (Company and Pierrot, 2002).

The inherent stiffness of the PKMs and higher speed (Taghirad, 2013) than the serial kinematic manipulators make them ideal for performing different tasks in the manufacturing sectors such as assembly and material processing (Schutz and Wahl, 2011).

The tasks of assembly, material processing as polishing or de-burring and material handling are tasks that require compliant motions (Bruyninckx and Schutter, 1996) i.e. the robot required to adapt the torques and forces when in contact with environmental objects.

An approach to compliant motion is the so called Impedance Control (Hogan, 1985). Impedance Control is classified as an indirect force control because is designed to avoid the necessity to measure the force in the mobile platform. The aim of Impedance Control is to impose a desired apparent mechanical stiffness and damping in the Cartesian space of the robot. In a robotic system that can perform 3 translations by 3 actuators, it becomes a straight forward task because

there is a one to one mapping from the Cartesian space to the actuator space. In a robotic system with actuator redundancy it is not a trivial task.

PKMs with redundant actuation are those that have more actuators than degrees of freedom. The control of redundant PKMs requires the solution of inverse dynamics which is not straight forward and techniques as the Moore-Penrose pseudo inverse matrix (Briot et al., 2013) or the null space of the forces is used (Kock and Schumacher, 2011) to solve this problem. There are advantages of redundant actuated robots such as improvement of Cartesian stiffness within the worspace, homogeneous symmetric force output and a need for optimization due to the fact that the dynamic equations are indeterminate (Cheng et al., 2001).

Recently, the BlueWorkforce company (Hjørnet, 2016) developed a new industrial redundant PKM (The Ragnar Robot) with an optimized extended workspace and relatively low price. By optimizing the mechanical design and force transmission it was possible to change materials and reduce costs.

The motivation behind the work presented in this paper is to introduce compliant motion control in redundantly actuated PKMs such as the Ragnar robot for optimization to perform different compliant motion tasks in a manufacturing environment.

In this paper, we proposed an impedance controller for a redundant parallel manipulator by setting a desired stiffness and damping for each coordinate axis in the cartesian space. The proposed method considers every limb as a separate system. Limb dy-

namic equations are coupled through internal interaction forces in the attachment points of the mobile platform. Impedance control is designed as a decoupled stiffness and damping for each direction of the coordinate axes.

The paper is organized as follows: In Section 2 the parallel kinematic manipulator is described. Section 3 briefly describes the kinematics of the manipulator. The dynamic model on which the impedance controller is based is described in Section 4. The trajectory generation and inverse dynamics of the redundant parallel robot is discussed in Section 5. The setting for the impedance controller and optimization is described in Section 6. In Section 7 simulations and results are presented for the proposed method. Section 8 presents a brief conclusion.

2 SYSTEM DESCRIPTION

The Ragnar parallel robot is a four limbs redundant parallel robot designed for 3D mobility of its mobile platform, while mechanically fixed in a constant orientation. Each limb comprises an actuated inner link attached to the base platform and an outer link attached to the mobile platform. The global coordinate system is located in the center of the base platform, the mobile coordinate system is located to the center of the mobile platform (center piece) and four auxiliary local coordinate systems are located to the connection between the mobile platform and each of the outer links. The figure shows the location of the global coordinate system, the mobile platform coordinate system and the first auxiliary coordinate system at the attachment point.
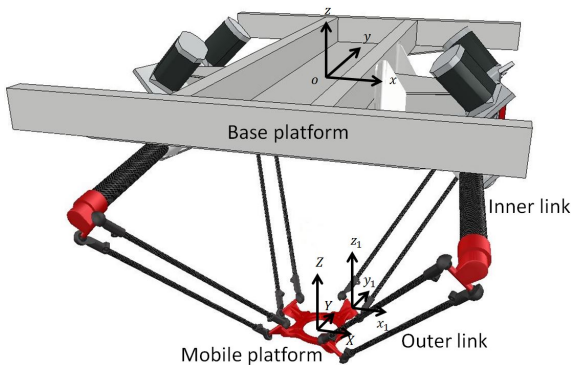

Figure 1: Ragnar robot with location of the coordinate systems.

3 KINEMATIC ANALYSIS

The kinematic constraint equations are given by a set of generalized coordinates q_i that can describe the position of one leg. The set of generalized coordinates chosen is composed by the active and passive joint angles of one limb, i.e. $q_i = \begin{bmatrix} \theta_i & \zeta_i & \eta_i \end{bmatrix}^T$. The active joint angle θ_i, passive joint angles ζ_i, η_i and geometric parameters are shown in the figure below.
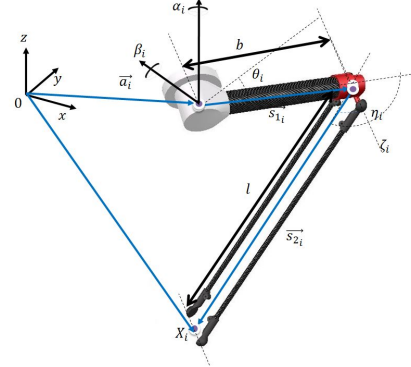

Figure 2: Generalized coordinates.

Let x_i denote the position of the i-th attachment point of the mobile platform and the limb. Then, the position vector of x_i in global coordinates is

$$\vec{a}_i + \vec{s}_{1_i} + \vec{s}_{2_i} = x_i \qquad (1)$$

Rewriting Eq. (1) in local vectors

$$\vec{a}_i + R_{1_i}\vec{b}_i + R_{1_i}R_{2_i}\vec{l}_i = x_i \qquad (2)$$

Where R_{1_i} denotes the rotation of the actuated joint and R_{2_i} the rotation of the passive joint

$$R_{1_i} = R_z^{\alpha_i} R_y^{\beta_i} R_z^{\theta_i} \qquad (3)$$

$$R_{2_i} = R_z^{\zeta_i} R_y^{\eta_i} \qquad (4)$$

where $\alpha_{1,3} = -\alpha_{2,4} = \pi/12$, $-\beta_{1,4} = \beta_{2,3} = \pi/4$ and the local vectors $\vec{b}_i$ and $\vec{l}_i$ defined as

$$\vec{b}_i = b_i\vec{i} \quad \vec{l}_i = l_i\vec{i} \qquad (5)$$

where $\vec{i}$ stands as the unit vector in the x direction of the i-th coordinate system. The solution to the inverse geometric problem is solved using a the well known spherical-spherical constraint (Garcia de Jalon and Bayo, 1994) and described in (Wu et al., 2016).

3.1 Jacobian Analysis

Differentiating Eq. (2) with respect to time we get the Jacobian for each separate limb.

$$\dot{x}_i = J_i\dot{q}_i \qquad (6)$$

with

$$J_i = \begin{bmatrix} j1_i & j2_i & j3_i \end{bmatrix} \tag{7}$$

where

$$j1_i = R_{1_i}\vec{k} \times \left(\vec{b}_i + R_{2_i}\vec{l}_i \right) \tag{8}$$

$$j2_i = R_{1_i}R_z^{\zeta_i}\vec{k} \times R_y^{\eta_i}\vec{l}_i \tag{9}$$

$$j3_i = R_{1_i}R_{2_i}\vec{j} \times \vec{l}_i \tag{10}$$

This allows to obtain four jacobians for a singular position that allow the calculation of all the velocities of the joints of the robot. Let x denote the position of the mobile platform, then its position can be described by

$$x = x_i + d_i \tag{11}$$

where d_i is a constant vector from the i-th attachment point to the mobile platform. Deriving Eq. (11) with respect to time yields

$$\dot{x} = \dot{x}_i \tag{12}$$

which implies

$$\dot{x} = J_i \dot{q}_i \tag{13}$$

4 DYNAMIC MODELING

The dynamic model is derived first in each limb and then are combined with the dynamic formulation of the mobile platform.

4.1 Dynamic Model of the Limb

The dynamics is computed using the variational method of the Lagrange equations.

The Lagrange equation is defined as

$$\frac{d}{dt}\left(\frac{\partial L_i}{\partial \dot{q}_i} \right) - \frac{\partial L_i}{\partial q_i} = Q_{ext_i} \tag{14}$$

And the Lagrangian

$$L_i \equiv T_i - V_i \tag{15}$$

where $Q_{ext_i} = \tau_i - J_i^T f_i$ are the external forces, $\tau_i = \begin{bmatrix} T_i & 0 & 0 \end{bmatrix}^T$ is the actuator torque and f_i is an interaction force in the attachment point. The center of mass of the inner link and the outer link are considered to be at the center of each link. Furthermore, the kinetic energy associated to the rotation of the outer link is deprecated for simplification. Figure 3 shows the external forces acting in the limb and Figure 4 shows the location of the center of mass of the limbs.

The kinetic energy T_i of the i-th limb is calculated as

$$T_i = \frac{1}{2}I_b\dot{\theta}_i^2 + \frac{1}{8}m_b\dot{\vec{s}}_{1_i}{}^2 + \frac{1}{2}m_l\left(\dot{\vec{s}}_{1_i} + \frac{1}{2}\dot{\vec{s}}_{2_i} \right)^2 \tag{16}$$
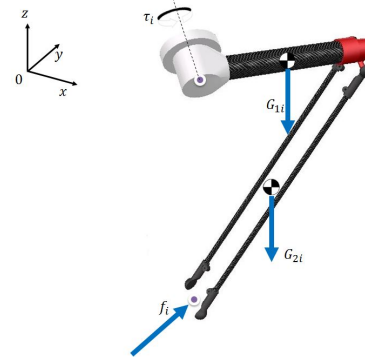

Figure 3: Torque, interaction force and gravity on the i-th limb.
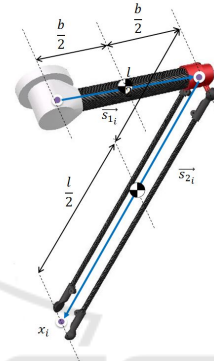

Figure 4: Center of mass of the links.

and the potential energy V_i of the i-th limb as

$$V_i = m_b\left(\frac{1}{2}\vec{s}_{1_i}{}^T \right)g + m_l\left(\vec{s}_{1_i} + \frac{1}{2}\vec{s}_{2_i} \right)^T g \tag{17}$$

where I_b and m_b is the inertia and mass of the inner link and m_l is the mass of the outer link.

Deriving the equations gives as a result an dynamic equation for the i-th limb in the form

$$M_i(q_i)\ddot{q}_i + C(\dot{q}_i, q_i) + G(q_i) = \tau_i - J_i^T f_i \tag{18}$$

4.2 Dynamic Model of the Mobile Platform

The rotation of the mobile platform is mechanically fixed, thus the dynamic equation is derived as

$$M_p\ddot{x} + G_p = f_e + \sum_{i=1}^{4} f_i \tag{19}$$

where $M_p = m_p I_3$ denotes the mass of the mobile platform times the identity matrix, f_i the effect of the interaction forces in the i-th attachment point G_p is the gravity vector of the mobile platform and f_e is the interface force between the mobile platform and the environment.

The full dynamic model of the robot is derived combining Eq. (18) and Eq. (19)
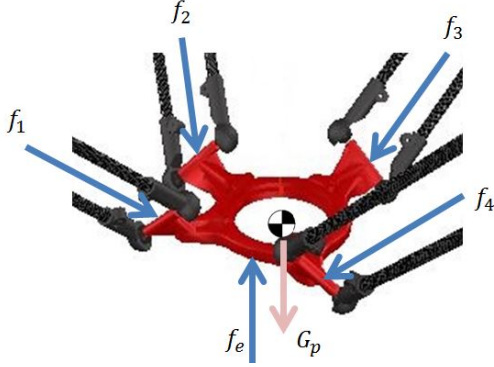
Figure 5: Forces acting on the mobile platform.

5 REFERENCE TRAJECTORY

The compliant motion of the robot is achieved when the robot deviates from its trajectory in response to the forces resulting from the robot interacting with an external object.

Given a reference trajectory as the set of positions, velocities and accelerations of the mobile platform i.e. $\{x_r, \dot{x}_r, \ddot{x}_r\}$, we can compute the set of positions, velocities and accelerations of the joints i.e. $\{q_{r_i}, \dot{q}_{r_i}, \ddot{q}_{r_i}\}$.

In a non-redundant robot, the torques of the motors can be determined through Eq. (18) and Eq. (19). In a redundantly actuated robot the torques for the motors cannot be determined directly through the dynamic equations. The inverse dynamics of the robot yields to three equations for translational motion and four torque inputs to be determined.

5.1 Reference Trajectory with Optimized Torques

The trajectory given in a set of the mobile platform and joints positions, velocities and accelerations $\{x_r, \dot{x}_r, \ddot{x}_r, q_{r_i}, \dot{q}_{r_i}, \ddot{q}_{r_i}\}$. The aim is to determine the value references of torques for the given trajectory.

The torque equation for a reference trajectory of the i-th limb becomes

$$\tau_{r_i} = M_i \ddot{q}_{r_i} + C(\dot{q}_{r_i}, q_{r_i}) + G(q_{r_i}) + J_{r_i}^T f_{r_i} \; \forall = 1..4 \tag{20}$$

and all the torque equations are combined with the translational motion equation of the mobile platform in absence of external forces, i.e.

$$M_p \ddot{x}_r + G_p = \sum_{i=1}^{4} f_{i_r} \tag{21}$$

Eqs. (21) and (20), given the reference trajectory form a set of 15 equations and 16 variables, thus the

solution for the inverse dynamics can have infinite solutions. The problem can be set as an optimization problem where the objective function can be selected, along with constraints, to support additional design specifications as well as to remove the ambiguity of the solution for actuator torques. In this paper the objective function is chosen to promote even distribution of the torques over actuators. We chose the objective function as follows

$$f_{obj}(f_i) = \sum_{i=1}^{4} T_i^2 \tag{22}$$

The optimization setting for finding the reference torques and forces, by combining Eq. (22), Eqs. (20) and Eq. (21) i.e.

$$min \; f_{obj}(f_i) \; \text{st}$$

$$M_p \ddot{x}_r + G_p - \sum_{i=1}^{4} f_{i_r} = 0$$

$$\tau_{r_i} = M_i \ddot{q}_{r_i} + C(\dot{q}_{r_i}, q_{r_i}) + G(q_{r_i}) + J_{r_i}^T f_i \; \forall i = 1..4$$

$$\tau_{r_i} = [T_{r_i} \; 0 \; 0]^T \; \forall i = 1..4$$

$$\underline{\tau} \leq \tau_{r_i} \leq \bar{\tau} \; \forall i = 1..4 \tag{23}$$

where $\underline{\tau}$ and $\bar{\tau}$ stand for the minimum and maximum torques of the motor. Defining

$$h_a \quad = \quad [1 \; 0 \; 0] \tag{24}$$

$$h_b \quad = \quad \begin{bmatrix} 0 & 1 & 0 \\ 0 & 0 & 1 \end{bmatrix} \tag{25}$$

we may reformulate Eq. (23) as

$$min_{f_1,...,f_4} \sum_{i=1}^{4} (h_a \tau_{r_i})^2 \; \text{st}$$

$$M_p \ddot{x}_r + G_p - \sum_{i=1}^{4} f_{i_r} = 0$$

$$h_b \tau_{r_i} = 0 \; \forall i = 1..4$$

$$\underline{\tau} - h_a \tau_{r_i} \leq 0 \; \forall i = 1..4$$

$$h_a \tau_{r_i} - \bar{\tau} \leq 0 \; \forall i = 1..4 \tag{26}$$

upon which reference torques T_{r_i} and internal interaction forces f_{r_i} are found.

6 IMPEDANCE CONTROL

Impedance control specifies a stiffness (k_p) and damping (k_v) to the mobile platform.

Taking Eq. (19) and renaming the sum of the internal interaction forces as a controlled forces f_c it can be re written as

$$M_p \ddot{x} + G_p = f_e + f_c + f_r \tag{27}$$

by subtracting

$$M_p \ddot{x}_r = f_r - G_p \qquad (28)$$

we obtain

$$M_p \delta \ddot{x} = f_e + f_c \qquad (29)$$

with

$$\delta x = x - x_r \qquad (30)$$

and set the desired damping and stiffness in the mobile platform, named the damping (K_p) and stiffness (K_v) matrices with a gravity compensator

$$f_c = -(K_p \delta x + P_v \delta \dot{x}) \qquad (31)$$

Inserting Eq. (31) into Eq. (27) we get

$$M_p \delta \ddot{x} = f_e - (K_p \delta x + K_v \delta \dot{x}) \qquad (32)$$

As a result, we obtain a relationship suitable for the design of an impedance controller, i.e.

$$M_p \delta \ddot{x} + K_v \delta \dot{x} + K_p \delta x = f_e \qquad (33)$$

The damping and stiffness matrices are usually chosen to be diagonal in order to decouple the dynamic effects in each direction of the Cartesian space.

6.1 Inverse Kinematics Approximation

Assuming that the robot position is sufficiently close to the reference trajectory the inverse kinematics approximate linearly as

$$\delta x_i = x_i - x_{r_i} \approx J_i(q_{r_i})(q_i - q_{r_i}) = J_i(q_{r_i}) \delta q_i \quad (34)$$

or

$$\delta q_i \approx J_i^{-1}(q_{r_i}) \delta x_i \qquad (35)$$

Defining

$$\mathcal{J}(t) = J_i^{-1}(q_{r_i}(t))$$

we obtain

$$\delta \dot{q}_i \approx \dot{\mathcal{J}} \delta x_i + \mathcal{J} \delta \dot{x}_i \qquad (36)$$

and

$$\delta \ddot{q}_i \quad \approx \quad \ddot{\mathcal{J}} \delta x_i + \dot{\mathcal{J}} \delta \dot{x}_i + \dot{\mathcal{J}} \delta \dot{x}_i + \mathcal{J} \delta \ddot{x}_i \qquad (37)$$
$$\approx \quad \ddot{\mathcal{J}} \delta x_i + 2 \dot{\mathcal{J}} \delta \dot{x}_i + \mathcal{J} \delta \ddot{x}_i \qquad (38)$$

We shall convert the limb i torque equation (18) into dynamics for x_i by a simplified linear approximation, i.e.

$$\delta \tau_i = \quad \tau_i - \tau_{r_i}$$
$$\approx \quad M(q_{r_i}) \delta \ddot{q}_{r_i} + G(q_{r_i})_q \delta q_i + J(q_{r_i}) \delta f_i \quad (39)$$

Finally, inserting Eq. (35), Eq. (36) and Eq. (38) into Eq. (39) we get an approximation of the limb i torque equation in terms of δx_i

6.2 Control Allocation

Similarly to Section 5 the problem is set up in an optimization. The torques are allocated through an optimization that promotes even distribution of torques, thus reducing the sudden change of manipulator torques. The optimization is set up using the objective function previously defined in Eq. (22), i.e.

$$min \ f_{obj}(f_i) \ st$$
$$K_p \delta x + K_v \delta \dot{x} + \sum_{i=1}^{4} f_i - G_p = 0$$
$$\delta \tau_i = M(q_{r_i}) \delta \ddot{q}_{r_i} + G(q_{r_i})_q \delta q_i + J(q_{r_i}) \delta f_i \ \ \forall i = 1..4$$
$$\tau_i = [T_i \ 0 \ 0]^T \ \forall i = 1..4$$
$$\underline{\tau} \leq \tau_i \leq \bar{\tau} \ \forall i = 1..4$$
$$\qquad (40)$$

and with further calculations

$$min \ \sum_{i=1}^{4} (h_a \ (\delta \tau_i + \tau_r))^2 \ st$$
$$K_p \delta x + K_v \delta \dot{x} + \sum_{i=1}^{4} f_i - G_p = 0$$
$$h_b \ (\delta \tau_i + \tau_r) = 0 \ \forall i = 1..4$$
$$\underline{\tau} - h_a \ (\delta \tau_i + \tau_r) \leq 0 \ \forall i = 1..4$$
$$h_a \ (\delta \tau_i + \tau_r) - \bar{\tau} \leq 0 \ \forall i = 1..4 \qquad (41)$$

where

$$T_i = \qquad h_a \ (\delta \tau_i + \tau_r) \qquad (42)$$
$$\delta \tau_i = \quad M(q_{r_i}) \delta \ddot{q}_{r_i} + G(q_{r_i})_q \delta q_i + J(q_{r_i}) \delta f_i \quad (43)$$

7 SIMULATION AND RESULTS

7.1 Simulation Setup

The masses and geometric parameters are taken from a CAD model of the robot. The controller and the dynamic model of the robot are simulated numerically. Table 1 shows the geometric and physical parameters of the robot.

7.1.1 Static Reference

The proposed method is evaluated, as the beginning of our investigation, in a static position ($\ddot{x}_r = \dot{x}_r = 0$) i.e. the reference trajectory. The reference position is the initial position of the robot, which is selected to be $x = [0 \ 0 \ -0.4]^T$. For the case of a non-static reference trajectory we can also apply the same procedure to find the reference forces and torques.

Table 1: Geometrical and physical parameters of the Ragnar Robot.

Parameter	Value
γ	$\frac{\pi}{6}$
a_i	$[\pm 0.28, \mp 0.114][m]$
α	$\frac{\pi}{12}$
b	$0.3[m]$
l	$0.55[m]$
r	$0.1[m]$
m_p	$0.25[kg]$
m_b	$0.3[kg]$
I_b	$0.0013[kg \cdot m^2]$
m_l	$0.12[kg]$
$max. torque$	$10[Nm]$

7.2 The Stiffness and the Damping Matrices

The stiffness and Damping matrices are selected to be diagonal in order to decouple the stiffness and damping responses in Cartesian space. We selected the following stiffness and damping matrices, for which the poles of each transfer function are different. We selected different stiffness gains for evaluation purposes and selected different cut-off (fr) frequencies for each axis to compute the damping.

$$K_p = \begin{bmatrix} K_{px} & 0 & 0 \\ 0 & K_{py} & 0 \\ 0 & 0 & K_{pz} \end{bmatrix} \quad (44)$$

$$K_v = \begin{bmatrix} K_{vx} & 0 & 0 \\ 0 & K_{vy} & 0 \\ 0 & 0 & K_{vz} \end{bmatrix} \quad (45)$$

Table 2: Stiffness and Damping design parameters.

Stifness	[N/m]	fr $[s^{-1}]$	Damping	[Ns/m]
K_{px}	1000	30	K_{vx}	40.83
K_{py}	500	10	K_{vy}	52.5
K_{pz}	200	5	K_{vz}	41.25

7.3 Step Response

A step response is applied to the system in each of the cartesian axis and is compared to the desired step response. The step input applied at $t = 0$ is $f_e = [1\ 1\ 1]^T$ The results are shown below.

It is observed that the step response of the simulation and the desired response is as expected with the largest error in the z-axis.

From the data of the simulation it was calculated the following constant of time for each of the step re-
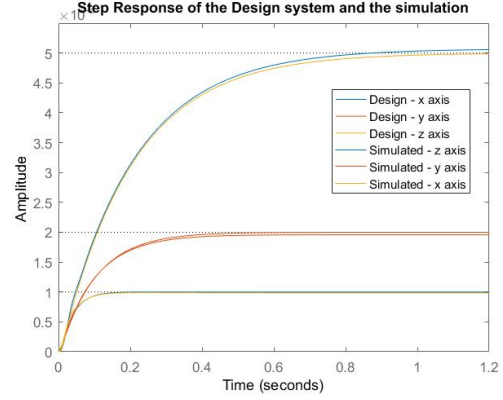

Figure 6: Step response of the simulation and the desired response.

sponses as

$$\tau_{t_x} = 0.0355 \quad (46)$$
$$\omega_x = 1/\tau_{t_x} = 28.16 \quad (47)$$
$$\tau_{t_y} = 0.096 \quad (48)$$
$$\omega_y = 1/\tau_{t_y} = 10.41 \quad (49)$$
$$\tau_{t_z} = 0.207 \quad (50)$$
$$\omega_z = 1/\tau_{t_z} = 4.83 \quad (51)$$

where the poles resulting from the selection of stiffness and damping in the design phase are

$$p_{x1} = -30 \qquad p_{x2} = -133.33 \quad (52)$$
$$p_{y1} = -10 \qquad p_{y2} = -200 \quad (53)$$
$$p_{z1} = -5 \qquad p_{z2} = -160 \quad (54)$$

We observed that the error of the measured cut off frequencies from the simulation, that correspond to the dominant poles, are very close to the design requirement. The measured absolute errors are

$$e_x = 1.84 \quad (55)$$
$$e_y = 0.41 \quad (56)$$
$$e_z = 0.17 \quad (57)$$

where the maximum error is measured in the x-axis possibly due to the approximations previously outlined.

7.4 Response to Harmonic Forces

In the last section a step response was applied to evaluate the desired response of the system against the simulation but is only valid for very low frequencies. The designed system is simulated for the case of external harmonic forces acting in the mobile platform. The harmonic forces are in the form

$$f_{he} = A\sin(2\pi \cdot \omega \cdot t) \quad (58)$$

An amplitude of $A = 1$ is selected for the harmonic forces and frequency is varied to obtain a sketch of the Bode plot of the simulated system with controller.

The external harmonic force is simulated as

$$f_e(t) = [f_{he} \ f_{he} \ f_{he}]^T$$

7.4.1 Bode Plot Comparison

Figures 7, 8 and 9 show the results from the simulation of the system when harmonic forces are applied to the mobile platform. The harmonic forces were applied in the direction of the three axis of the global coordinate system. Then, the gain was computed from the simulation. Different frequencies were applied to the system to test the controller and obtain the Bode plot of the system with the controller.

Comparing the response to harmonic forces in different frequencies we observe that the cut-off frequency is almost half decade behind the designed cut off frequency. This can be caused due to the small difference of the mass of the mobile platform and the limbs, which does not allow for many simplifications
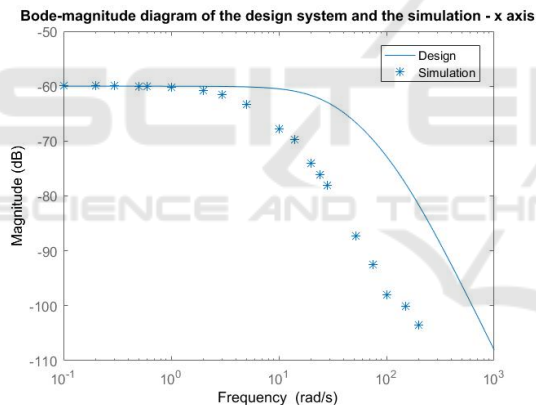

Figure 7: Bode plot of the simulation and the desired response in x-axis.
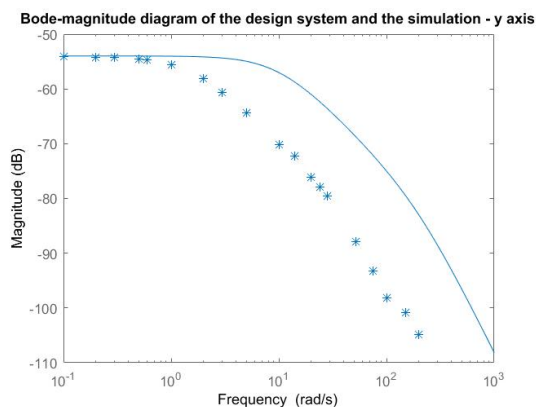

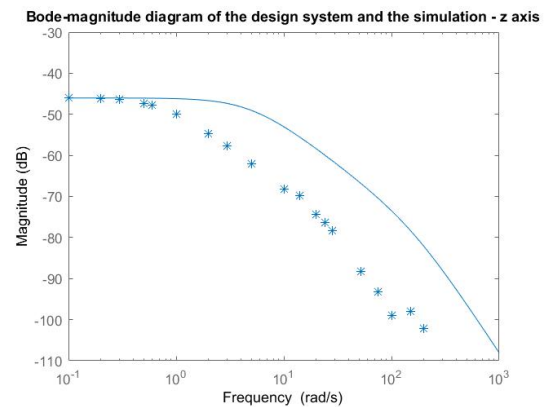Figure 8: Bode plot of the simulation and the desired response in y-axis.

Figure 9: Bode plot of the simulation and the desired response in z-axis.

but could be mitigated when the mass of the mobile platform is increased when there is a tool attached to it.

8 CONCLUSIONS

In this paper was presented the case for impedance control for a redundant parallel robot. The impedance control is based on linearisation of the robot dynamics around a reference trajectory. We showed that the controller works in a region close to the reference trajectory and its response to harmonic forces differs to the design but the step response is as designed with small error but it increases when the stiffness or damping is reduced. The simulation showed that the system has a time constant similar to the design requirement on each axis.

Since the Ragnar robot is a redundantly actuated parallel robot, its inverse dynamics is indeterminate and an optimization is applied to obtain torques. Future work includes the implementation of the designed controller on the Ragnar robot as well as applying the compliance approach presented in this paper in an iterative learning framework for improved performance in eg. assembly.

REFERENCES

Briot, S., Gautier, M., and Krut, S. (2013). Dynamic parameter identification of actuation redundant parallel robots: Application to the dualv. In *AIM: Advanced Intelligent Mechatronics, Jul 2013, Wollongong, Australia. IEEE/ASME*, pages pp.637–643.

Bruyninckx, H. and Schutter, J. D. (1996). Specification of force-controlled actions in the ldquo;task frame formalism rdquo;-a synthesis. *IEEE Transactions on Robotics and Automation*, 12(4):581–589.

Cheng, H., Liu, G. F., Yiu, Y. K., Xiong, Z. H., and Li, Z. X. (2001). Advantages and dynamics of parallel manipulators with redundant actuation. In *Proceedings 2001 IEEE/RSJ International Conference on Intelligent Robots and Systems. Expanding the Societal Role of Robotics in the the Next Millennium (Cat. No.01CH37180)*, volume 1, pages 171–176 vol.1.

Company, O. and Pierrot, F. (2002). Modeling and design issues of a 3-axis parallel machine tool. In *Mechanism and Machine Theory, Vol. 37, No. 11*, pages 1325–1345.

Garcia de Jalon, J. and Bayo, E. (1994). *Kinematic and Synamic Simulation of Multibody Systems*. Springer-Verlag New York.

Hjørnet, P. (2016). Blueworkforce home page. http://blueworkforce.com/.

Hogan, N. (1985). Impedance control: An approach to manipulation: Part itheory. In *ASME. J. Dyn. Sys., Meas., Control.*, pages 107(1):1–7.

Kock, S. and Schumacher, W. (2011). *Redundant Parallel Kinematic Structures and Their Control*, pages 143–157. Springer Berlin Heidelberg, Berlin, Heidelberg.

McCallion, H. and Pham, D. (July 1979). The analysis of a six degrees of freedom work station for mechanized assembly. In *In Proc. 5th World Congress on Theory of Machines and Mechanisms*, page 611616, Montreal.

Ming, A. and Higuchi, T. (September 1994). Study on multiple degree of freedom positioning mechanisms using wires, part 2, development of a planar completely restrained positioning mechanism. In *Int. J. Japan Soc. Prec.Eng.*, page 28(3):235242.

Patel, Y. and George, P. (2012). Parallel manipulators applications a survey. In *Modern Mechanical Engineering*, pages pp. 57–64.

Powell, I. (Third Quarter 1982). The kinematic analysis and simulation of the parallel topology manipulator. In *The Marconi Review*, page XLV(226):121138.

Salcudean, S. et al. (1994). A six degree-of-freedom, hydraulic, one person motion simulator. In *In IEEE Int. Conf. on Robotics and Automation*, page 24372443, San Diego.

Schutz, D. and Wahl, F. M. (2011). *Robotic Systems for Handling and Assembly*, volume 67. Springer Berlin Heidelberg.

Taghirad, H. D. (2013). *Parallel Robots: Mechanics and Control*. CRC Press.

Wu, G., Bai, S., and Hjørnet, P. (2016). Architecture optimization of a parallel schönflies-motion robot for pick-and-place applications in a predefined workspace. *Mechanism and Machine Theory*, 106:148 – 165.